Research Article

For reprint orders, please contact: reprints@futuremedicine.com

Nanomedicine

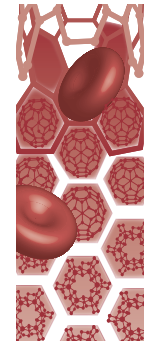

Bioactive nanoparticles improve calcium handling in failing cardiac myocytes

Aims: To evaluate the ability of *N*-acetylglucosamine (GlcNAc) decorated nanoparticles and their cargo to modulate calcium handling in failing cardiac myocytes (CMs). **Materials & methods:** Primary CMs isolated from normal and failing hearts were treated with GlcNAc nanoparticles in order to assess the ability of the nanoparticles and their cargo to correct dysfunctional calcium handling in failing myocytes. **Results & conclusion:** GlcNAc particles reduced aberrant calcium release in failing CMs and restored sarcomere function. Additionally, encapsulation of a small calcium-modulating protein, S100A1, in GlcNAc nanoparticles also showed improved calcium regulation. Thus, the development of our bioactive nanoparticle allows for a 'two-hit' treatment, by which the cargo and also the nanoparticle itself can modulate intracellular protein activity.

Keywords: biomolecules • calcium handling • cardiac myocytes • encapsulation • GlcNAc • heart failure • nanoparticles • S100A1

Joshua T Maxwell[1,2,3], Inthirai Somasuntharam[1], Warren D Gray[1], Ming Shen[2,3], Jason M Singer[2,3], Bo Wang[2,3], Talib Saafir[2,3], Brian H Crawford[2,3], Rong Jiang[2,3], Niren Murthy[4], Michael E Davis[‡,1,2,3] & Mary B Wagner*[,‡,2,3]

[1]Wallace H Coulter Department of Biomedical Engineering, Emory University School of Medicine, 1648 Pierce Dr NE, Atlanta, GA 30307, USA

[2]Division of Pediatric Cardiology, Department of Pediatrics, Emory University School of Medicine, 1648 Pierce Dr NE, Atlanta, GA 30307, USA

[3]Children's Heart Research & Outcomes (HeRO) Center, Children's Healthcare of Atlanta & Emory University, Atlanta, GA, USA

[4]Department of Bioengineering, University of California Berkeley, Berkeley, CA, USA

*Author for correspondence: mary.wagner@emory.edu

[‡]Authors contributed equally

Heart failure (HF) is a complex pathological process that can be simply defined at the organ level as a decrease in cardiac function. In HF, profound disturbances in calcium (Ca^{2+}) signaling and excitation-contraction (E-C) coupling lead to compromised contractility and an increased propensity of arrhythmia. The reduction in contractility is in part due to the substantial decrease in sarcoplasmic/endoplasmic reticulum (SR) Ca^{2+} release during E-C coupling through the major SR-Ca^{2+} release channel in the heart, the RyR2 [1–3]. In response, post-translational modifications to the RyR2 can sensitize the channel to Ca^{2+} activation during systole, however, the modifications also increase the SR Ca^{2+} leak during diastole [4–6]. Spontaneous Ca^{2+} release events such as Ca^{2+} sparks and Ca^{2+} waves become more frequent and make the compensatory modifications potentially arrhythmogenic [7].

During the progression of HF, changes in protein expression lead to a multitude of remodeling processes and alterations in the function of single cardiomyocytes (CMs) and the heart as a whole. The correction of dysregulated protein levels of important Ca^{2+} handling proteins in HF have provided a therapeutic target for many years. Recently, the cardiac Ca^{2+}-binding protein S100A1 has emerged as an attractive therapeutic target based on its interaction with E-C coupling proteins including SERCA2a, PLB and the RyR2 [8–10]. Due to its ability to bind and modulate these critical Ca^{2+} handling proteins, S100A1 has become the basis for ongoing preclinical trials for HF therapy [11,12]. Although promising, these trials still lack the efficacy and specificity necessary for a viable therapeutic strategy to correct the pathological effects of HF. One major limitation is that S100A1 is unable to cross the cell membrane and thus intracellular delivery remains a major hurdle.

Our laboratory has previously described the development of a small molecule delivery system for enhanced CM uptake. By decorating degradable, biocompatible polymeric nanoparticles (polyketals) with *N*-acetylglucosamine (GlcNAc), rapid and

Future Medicine part of fsg

efficient internalization by CMs and functional effects of the delivered cargo were shown [13]. In cells, the enzyme *O*-GlcNAc transferase catalyzes attachment of GlcNAc to serine or threonine residues of proteins, which in CMs include key intracellular [Ca^{2+}] regulating proteins such as SERCA2a, CaMKII, PLB and STIM1 (reviewed in [14]). Thus, in the present study, in addition to facilitating the delivery of functional small molecules and proteins to CMs, we proposed that the GlcNAc molecule released from intracellular nanoparticle degradation can be used as a substrate for post-translational modification of calcium handling proteins in CMs, hence making it a 'bioactive' nanoparticle. We hypothesized that the GlcNAc nanoparticles would have a 'two-hit' effect on Ca^{2+} handling in CMs whereby the cargo and also the GlcNAc moiety itself can modulate intracellular protein activity. To test this hypothesis, we utilized CMs isolated from rats with right ventricular HF induced by pulmonary artery banding (PAB) and assessed various physiological Ca^{2+} handling parameters. After treatment with either empty-GlcNAc or S100A1-GlcNAc nanoparticles, we observed a decrease in the amplitude and frequency of arrhythmogenic Ca^{2+} release in the form of Ca^{2+} sparks. Additionally, we recorded an increase in electrically induced Ca^{2+} transient amplitude, an increase in cell shortening and a decrease in the diastolic Ca^{2+} in the cytosol after treatment with either empty-GlcNAc or S100A1-GlcNAc nanoparticles. These data indicate that GlcNAc nanoparticles are suitable vehicles for efficient delivery of small molecules to CMs, and the empty-GlcNAc nanoparticles are themselves biologically active and able to regulate the Ca^{2+} handling proteins in CMs. Thus, we report the development of a bioactive nanoparticle that provides a 'two-hit' treatment to CMs that can be utilized for further encapsulation of therapeutic molecules and proteins for efficient delivery to CMs.

Materials & methods

Solutions & chemicals

All chemicals and reagents were purchased from Sigma-Aldrich (MO, USA) unless otherwise stated. Fluorescent Ca^{2+} indicator dyes were purchased from Molecular Probes/Invitrogen (CA, USA). S100A1 recombinant protein was purchased from Creative Biomart (NY, USA), reconstituted in water at 0.5 µg/µl, and stored at -80°C until use. Tyrode's solution contained (in mM) 138 NaCl, 4 KCl, 2 $CaCl_2$, 1 $MgCl_2$, 10 glucose and 10 HEPES; pH 7.4 with NaOH.

Nanoparticle production

Polyketal particles loaded with (9′-(4-(and 5)-chloromethyl-2-carboxyphenyl)-7′-chloro-6′oxo-1,2,2,4-tetramethyl-1,2-dihydropyrido[2′,3′-6]xanthene) (CMRA) or S100A1 protein were generated using an emulsion-solvent evaporation technique previous described [13]. Briefly, 40 mg of poly(cyclohexane-1,4-diyl acetone dimethylene ketal) (PCADK) and cargo (100 µg CMRA or 50 µg S100A1) were dissolved in 1 ml of dichloromethane. Cargo volume in empty particle production was replaced with water. The polymer solution was added to 5 ml of 5% polyvinyl alcohol with or without 5 mg GlcNAc-alkyl, homogenized at high speed for 60 s, and sonicated for 30 s to produce nanoparticles. The resulting emulsion was transferred to 40 ml of 0.5% polyvinyl alcohol and stirred for 4 h at 100 rpm to evaporate solvent. Particle suspensions were centrifuged at 15,000 rpm for 15 min and washed with deionized water three times. The final pellet was resuspended in 3 ml deionized water, snap frozen in liquid nitrogen, lyophilized, and stored at -80°C.

Rat pulmonary artery banding model

Nonischemic heart failure was induced in male Sprague-Dawley rats by banding of the pulmonary artery as previously described [15]. Briefly, rats were anesthetized and the chest was open via a left thoracotomy to expose the heart. The pericardium was opened and the pulmonary artery was partially ligated over an 18 gauge angiocatheter to ensure consistent stenosis. The sizer was promptly removed to allow for antegrade flow through the banded area and the thoracotomy was closed under positive pressure ventilation to evacuate pleural air. Similarly, sham operated animals underwent the same procedure with exposure of the pulmonary artery but without banding.

Myocyte isolation

Single ventricular myocytes were isolated from sham and PAB rats. Rats were anesthetized with ketamine (0.1 mg/g) and xylazine (0.01 mg/g), and hearts were excised and mounted on a Langendorff apparatus. Hearts were retrogradely perfused with nominally Ca^{2+}-free Tyrode's solution for 5 min followed by Minimal Essential Medium Eagle (MEM) solution containing 20 µM Ca^{2+} and 22.5 µg/ml Liberase Blendzyme TH (Roche Applied Science, IN, USA) for 25–45 min at 37°C. The right ventricular free wall was removed from the heart, minced, filtered and washed in MEM solution containing 50 µM Ca^{2+} and 10 mg/ml bovine serum albumin. Isolated cells were kept in MEM solution with 50 µM Ca^{2+} at room temperature (22–24°C) until indicator dye loading and subsequent experimentation. All protocols were approved by the Institutional Animal Care and Use Committee.

CM nanoparticle treatment, CMRA fluorescence & flow cytometry

All particles were resuspended in Tyrode's solution at a concentration of 0.5 mg/ml. Rat CMs were incubated at 37°C with either polyketal particles loaded with CMRA or polyketal particles decorated with GlcNAc and loaded with CMRA. Cells were sampled at 15–30 min intervals and imaged. CMRA uptake was quantified by fluorescence intensity utilizing confocal microscopy with microscope and laser settings kept constant for all imaging (Fluoview 1000, Olympus Corporation, Japan). Cells were collected after 2 h of treatment and analyzed by flow cytometry for the presence of CMRA fluorescence. Data were analyzed using Flow Jo v10 software. For calcium handling studies, rat CMs were incubated for 1 h at 37°C with empty-GlcNAc nanoparticles or S100A1 nanoparticles prior to Ca^{2+} indicator loading.

Ca^{2+} spark measurements

Confocal microscopy (Fluoview 1000, Olympus Corporation, Japan) was used to image Ca^{2+} sparks, with excitation at 488 nm and emission collected at >500 nm. Cardiac myocytes were loaded with 20 µm fluo-4/AM for 20 min at room temperature, followed by a 20 min wash in 0 Ca^{2+} Tyrode's at room temperature. Ca^{2+} spark measurements were acquired from intact myocytes perfused with Tyrode's solution during rest after 1 Hz stimulation in line scan mode at 2 ms/line with a pixel size of 0.155 µm. The native protein treatment group contained 0.1 µm native S100A1 in the Tyrode's solution. All fluorescent signals were background subtracted. Changes in $[Ca^{2+}]_i$ are expressed as $\Delta F/F_0$, where ΔF is the change in fluorescence (measured fluorescence $[F] - F_0$) and F_0 is resting baseline fluo-4 fluorescence. For all subsequent Ca^{2+} imaging experiments, cells were placed on laminin-coated coverslips. Action potentials and global Ca^{2+} transients were elicited by electrical field stimulation using a pair of platinum electrodes. Experiments were conducted at room temperature (22–24°C).

Permeabilized cell solutions & Ca^{2+} spark measurements

Calcium sparks were recorded from ventricular myocytes after permeabilization with 0.05% Saponin. Cells were bathed in an internal solution composed of (in mM): 100 Potassium Aspartate, 15 KCl, 5 KH_2PO_4, 5 MgATP, 0.35 EGTA, 0.12 $CaCl_2$, 0.75 $MgCl_2$, 10 Phosphocreatine, 0.04 fluo-4 pentapotassium salt. This resulted in a $[Ca^{2+}]_{FREE}$ of 150 nM (calculated using Maxchelator, Stanford University). The internal solution for the S100A1 treatment group also contained 0.1 µM de-encapsulated S100A1 protein. Spark measurements were acquired as described above and reported as $\Delta F/F_0$.

Intracellular Ca^{2+} concentration & cell shortening measurements

Global intracellular Ca^{2+} concentration $[Ca^{2+}]_i$ and cell shortening were measured with an IonOptix Myocyte Calcium Photometry and Contractility System (MA, USA). Intracellular Ca^{2+} was monitored by fluorescent microscopy in single intact myocytes using the ratiometric dye fura-2/AM, with dye excitation at 340 nm (F_{340}) and 380 nm (F_{380}) and emission collected at 510 nm. F_{340} and F_{380} signals were background subtracted and changes in $[Ca^{2+}]$ are expressed as follows: $R = F_{340}/F_{380}$, where R is the ratio of the fluorescence signals F_{340} and F_{380}. The action potential-induced Ca^{2+} transient amplitude was defined as follows: $\Delta R = R_{peak} - R_{diast}$, where R_{peak} is the peak R signal and R_{diast} is the minimum R signal before the Ca^{2+} transient. Sarcomere shortening was measured by Fourier analysis of the myocyte image in real time [16].

Immunoprecipitation & western blot

Freshly isolated rat right ventricular myocytes were plated and incubated with vehicle or PK nanoparticles for 2 h at 37°C. Cells were harvested and lysed in lysis buffer (in mM: 25 Tris, 150 NaCl, 1 EDTA, 1% NP-40, 5% glycerol, pH 7.4). The protein concentration of the lysate was determined with the BCA Protein Assay (Thermo Fisher Scientific, Waltham, MA, USA), 10 µg of the immunoprecipitating antibody anti-SERCA2a (Santa Cruz Biotechnology, Dallas, TX, USA), anti-RyR2 (34C, Life Technologies, Grand Island, NY, USA) or anti-PLB (Life Technologies, Grand Island, NY, USA) were added to 500 µg of cell lysate and incubated overnight at 4°C with agitation. Then 30 µl of a 10% slurry of protein A-Sepharose CL-4B beads (Amersham Biosciences, Piscataway, NJ, USA) were added and incubated for 2 h at 4°C with agitation. Immune complexes were then washed three-times with lysis buffer, treated with SDS-PAGE sample buffer, boiled for 5 min, resolved on SDS-PAGE and transferred to nitrocellulose membrane. Membranes were incubated with either anti-*O*-GlcNAc or anti-SERCA2a, anti-RyR2 or anti-PLB antibody followed by incubation with HRP-conjugated secondary antibody. Visualization was accomplished using ECL reagents (GE Healthcare, Piscataway, NJ, USA).

Data presentation & statistics

Line scan data and fluorescence traces are presented as individual observations representative of multiple recordings. Summary data are presented as the mean ± SD of n measurements. Statistical compari-

sons between groups were performed with one-way ANOVA with Tukey's posthoc test. Differences were considered statistically significant at $p < 0.05$.

Results

GlcNAc decoration increases polyketal nanoparticle uptake in isolated failing cardiac myocytes

To compare the transfer of cargo to target cells by polyketal nanoparticles with and without GlcNAc decoration on their surface, we examined the time course of uptake between nondecorated and GlcNAc-decorated nanoparticles in failing CMs. To do this, we loaded both nondecorated nanoparticles and GlcNAc-decorated nanoparticles with CMRA, a fluorophore that does not fluoresce until it is taken up by cells. CMs treated with nondecorated nanoparticles (PK-CMRA) exhibited very little uptake as measured by CMRA fluorescence (Figure 1A). CMs treated with GlcNAc-decorated nanoparticles (PK-GlcNAc-CMRA), however, showed a rapid increase of cellular fluorescence within the first 45 min of particle treatment. The fluorescence plateaued around this time point after reaching a fluorescence intensity approximately 1.5-times the baseline intensity. Representative images of CMRA fluorescence in CMs at various time points of nanoparticle treatment are shown in Figure 1B. CMs treated with GlcNAc-decorated nanoparticles showed a significant increase in CMRA fluorescence compared with nondecorated particles after approximately 20 min of treatment. Additionally, flow cytometry was used to quantify nanoparticle uptake in CMs after 2 h of treatment. Figure 1C shows a representative histogram demonstrating nearly 90% uptake in cells treated with PK-GlcNAc-CMRA particles compared with cells treated with PK-CMRA particles. These data show that GlcNAc decoration increases polyketal nanoparticle uptake in isolated CMs and efficient cargo protein delivery is achieved. It is important to note here that our polyketal nanoparticles degrade into biocompatible products and have been shown to neither incite the inflammatory response nor induce cell death [13,17,18].

S100A1 cargo protein retains its physiological function after nanoparticle degradation

Our nanoparticles are composed of the polyketal PCADK that degrades in acidic environments such as the developing endosome. In order to assure our cargo protein retains function after intracellular particle degradation, S100A1 recombinant protein was encapsulated within our polyketal nanoparticles, and the S100A1 nanoparticles were treated with 1 N HCl to degrade the PCADK *in vitro*. This reaction was stopped with the addition of an equal volume of 1 N NaOH. This mixture was then added to the internal solution used to measure Ca^{2+} sparks to give a final concentration of 0.1 μM free S100A1 de-encapsulated protein. We utilized right ventricular myocytes isolated from rats with nonischemic HF induced by PAB causing pressure overload and sham-operated rats to determine the effect of de-encapsulated S100A1 treatment on Ca^{2+} spark properties. Saponin permeabilized PAB myocytes were bathed in internal solution with and without de-encapsulated S100A1 and calcium sparks were measured in these cells, sham myocytes were used as control. Ca^{2+} sparks are elementary SR Ca^{2+}-release events through a cluster of RyR2s that occur spontaneously during diastole and summate in time and space during systole to form the global Ca^{2+} transient during E-C coupling [19]. To monitor rapidly changing phenomena such as fluorescence signals from Ca^{2+} sparks, the scan speed or frame rate becomes critical thus laser scanning confocal microscopes are utilized to acquire a row of pixels along a single axis of the specimen over time. These line scans enable visualization of rapid fluorescence intensity changes with time. Representative line scans of Ca^{2+} sparks acquired from the three groups of cells are shown in Figure 2A, and the properties of these events were analyzed and summarized in Figure 2B–E. PAB myocytes exhibited an increased spark frequency compared with permeabilized sham cells (CTL; Figure 2C). When the internal solution containing the de-encapsulated S100A1 was used, the spark frequency in the PAB myocytes was significantly decreased to nearly CTL levels (PAB + S100A1; Figure 2C). Treatment of PAB myocytes with de-encapsulated S100A1 also significantly decreased the amplitude, full width at half maximum (FWHM) and the full duration at half maximum (FDHM) of Ca^{2+} sparks compared with untreated PAB myocytes (Figure 2B–E) consistent with a previous report using permeabilized rabbit ventricular myocytes and exogenously supplied S100A1 native protein [20]. These data indicate that the encapsulation and de-encapsulation processes do not alter the function of the cargo protein.

GlcNAc nanoparticles decrease the frequency of Ca^{2+} sparks in intact PAB myocytes

After confirming GlcNAc decoration facilitates particle uptake into CMs and functional protein is released, we examined the effect of GlcNAc particles on several aspects of Ca^{2+} handling in intact CMs. Ca^{2+} sparks were recorded from untreated PAB myocytes or PAB myocytes treated with empty-GlcNAc particles, S100A1-GlcNAc particles or nonencapsulated S100A1 native protein. Representative line scans of Ca^{2+} sparks from these groups are shown in Figure 3A. Treatment

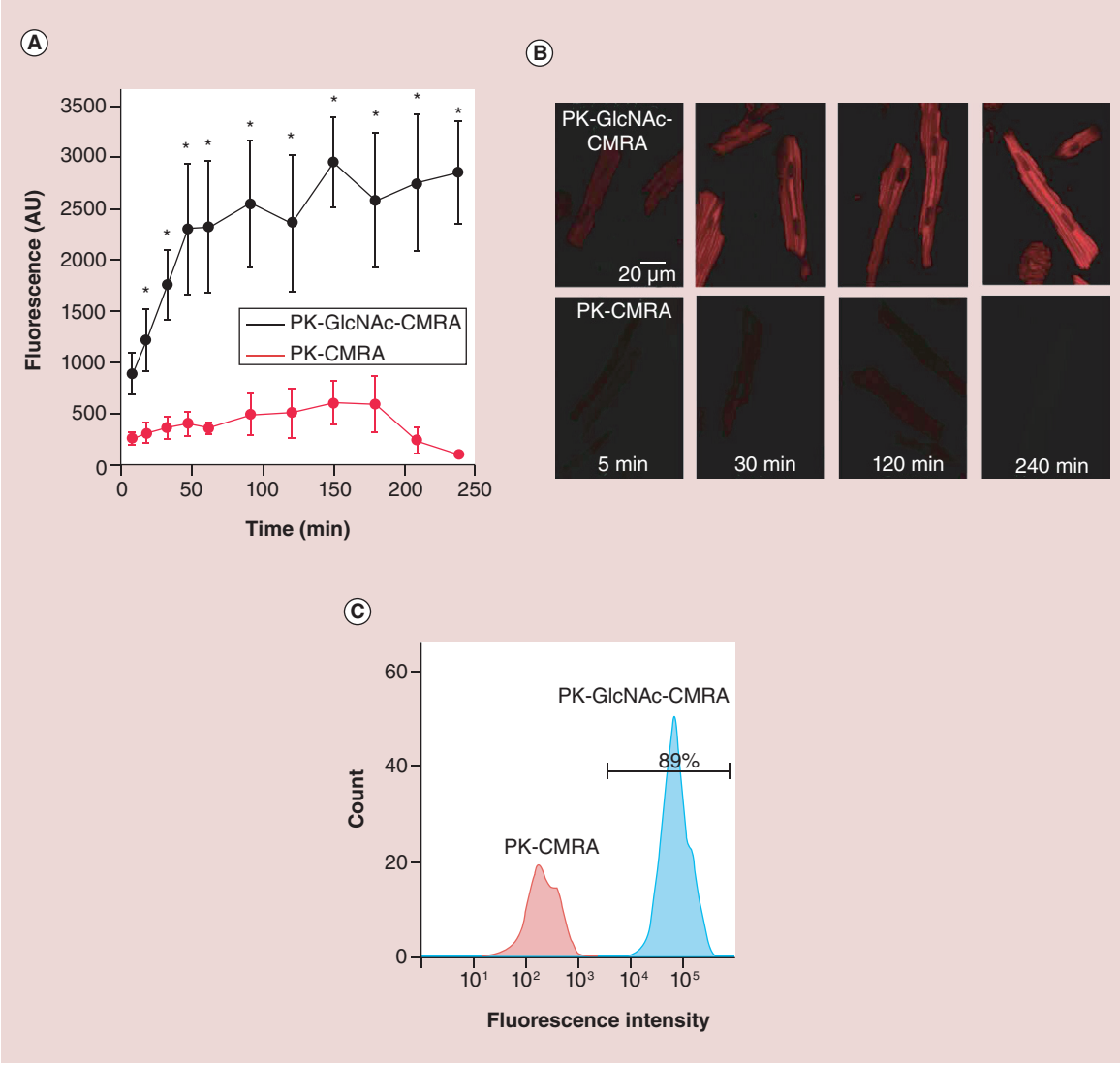

Figure 1. *N*-acetylglucosamine decoration increases uptake in isolated cardiac myocytes. CMs were incubated with CMRA-loaded GlcNAc decorated particles (PK-GlcNAc-CMRA) or undecorated particles (PK-CMRA) and imaged for individual cell quantification of CMRA fluorescence at various time points after particle application. **(A)** Summary data plot shows the average intracellular CMRA fluorescence intensity over time for PK-GlcNAc-CMRA (black) and PK-CMRA (red). n = 8–15 cells from n = 2 rats; *p < 0.05. **(B)** Representative fluorescent images of cells incubated with PK-GlcNAc-CMRA (top panels) or PK-CMRA (bottom panels) for 5, 30, 120 and 240 min. **(C)** Representative histograms of CMRA-positive cells. The area under the black bar is indicative of the percentage of cells exhibiting CMRA fluorescence as quantified by flow cytometry.
CM: Cardiac myocytes; CMRA: (9′-[4-(and 5)-chloromethyl-2-carboxyphenyl]-7′-chloro-6′oxo-1,2,2,4-tetramethyl-1,2-dihydropyrido[2′,3′-6]xanthene).

of PAB myocytes with empty-GlcNAc nanoparticles was able to significantly decrease the amplitude, frequency and FWHM of these events compared with untreated PAB cells (Figure 3B–D). Treatment of PAB myocytes with either empty-GlcNAc or S100A1-GlcNAc nanoparticles did not have an effect on the FDHM of Ca^{2+} sparks in these cells (Figure 3E). These results combined with the results from Figure 1 indicate a facilitation of cargo protein uptake by encapsulation in GlcNAc nanoparticles and illustrate the ability of GlcNAc nanoparticles and S100A1 cargo protein to modulate Ca^{2+} release events in intact CMs.

GlcNAc nanoparticles correct dysfunction in global Ca^{2+} handling & contractile function in PAB myocytes

Contractility and $[Ca^{2+}]_i$ measurements were made in untreated PAB myocytes or PAB myocytes treated with empty-GlcNAc particles or S100A1-GlcNAc particles. Representative sarcomere shortening (Figure 4A), Ca^{2+}

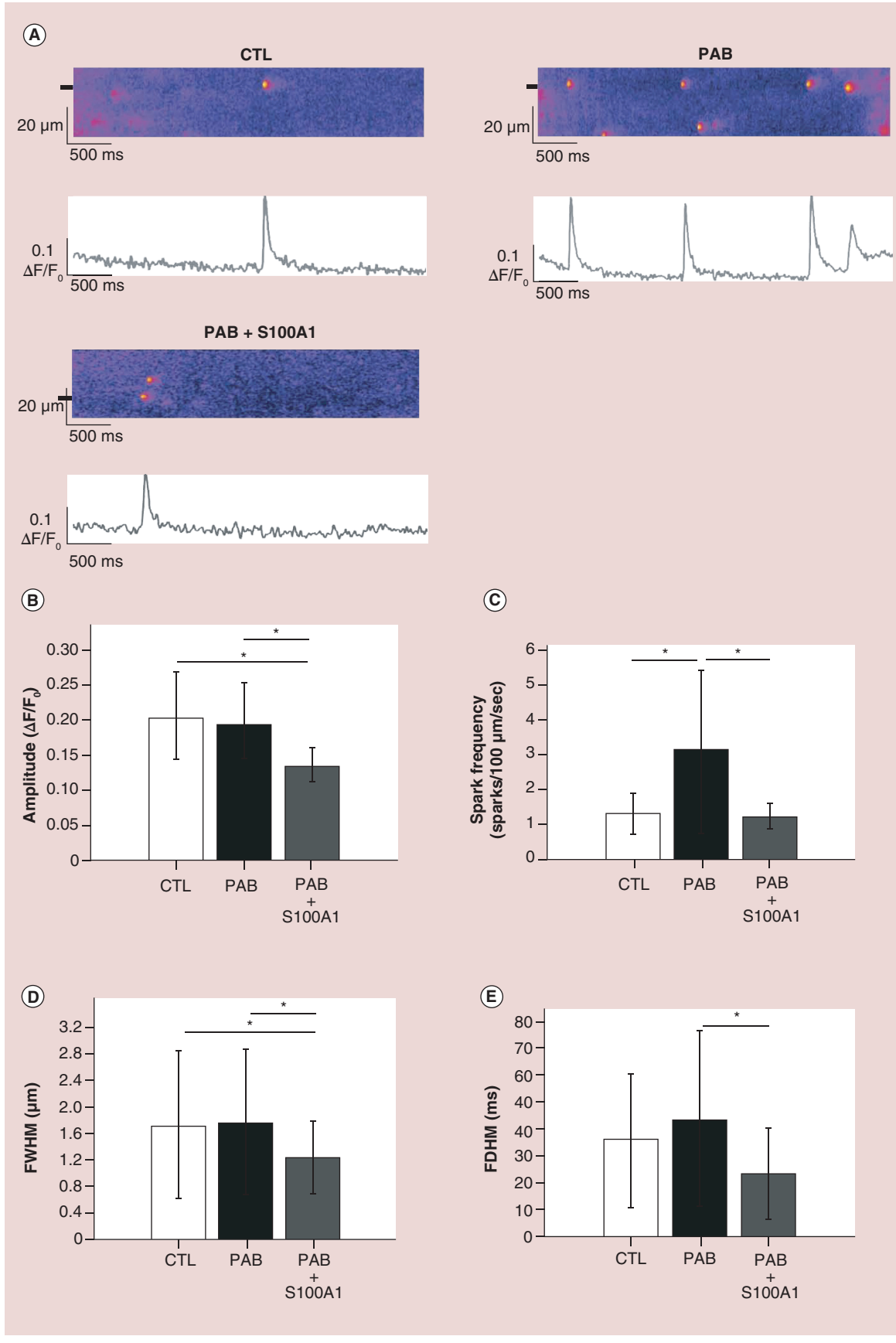
A
CTL
20 µm
500 ms
0.1
ΔF/F0
500 ms
PAB
20 µm
500 ms
0.1
ΔF/F0
500 ms
PAB + S100A1
20 µm
500 ms
0.1
ΔF/F0
500 ms
B
Amplitude (ΔF/F0)
0.30
0.25
0.20
0.15
0.10
0.05
0
CTL
PAB
PAB + S100A1
C
Spark frequency (sparks/100 µm/sec)
6
5
4
3
2
1
0
CTL
PAB
PAB + S100A1
D
FWHM (µm)
3.2
2.8
2.4
2.0
1.6
1.2
0.8
0.4
0
CTL
PAB
PAB + S100A1
E
FDHM (ms)
80
70
60
40
40
30
20
10
0
CTL
PAB
PAB + S100A1

Figure 2. De-encapsulated S100A1 alters Ca^{2+} spark properties from permeabilized right ventricular myocytes (see facing page). **(A)** Representative confocal line scans and the corresponding fluorescence profiles ($\Delta F/F_0$) of Ca^{2+} sparks from permeabilized rat myocytes from CTL, PAB or PAB treated with de-encapsulated S100A1 (PAB + S100A1). Fluorescent profiles were generated from the line scan regions marked by black boxes. **(B–D)** Summary data of the spark amplitude **(B)**, spark frequency **(C)**, full width at half maximum **(D)** and full duration at half maximum **(E)** measured from the three groups. CTL: n = 80 sparks from n = 7 rats; PAB: n = 212 sparks from n = 10 rats; PAB + S100A1: n = 33 sparks from n = 9 rats.
*$p < 0.05$.
CTL: Control; PAB: Pulmonary artery banding.

transient amplitude (Figure 4B) and diastolic $[Ca^{2+}]_i$ (Figure 4C) traces during electrical stimulation are shown above the summary data bar graphs in Figure 4. In PAB cells, treatment with either empty-GlcNAc or S100A1-GlcNAc nanoparticles nearly doubled the percent of sarcomere shortening compared with untreated PAB myocytes at both 0.5 and 1 Hz stimulation frequencies (Figure 4A). Additionally, PAB myocytes showed a significant increase in Ca^{2+} transient amplitude following empty-GlcNAC nanoparticle treatment, while a smaller yet still significant increase was seen with S100A1-GlcNAc treatment (Figure 4B). Diastolic $[Ca^{2+}]_i$ measurements were also recorded from PAB myocytes under control conditions or after incubation with either empty-GlcNAc or S100A1-GlcNAc particles (Figure 4C). As summarized in the bar graph below the traces, treatment with both empty-GlcNAc and S100A1-GlcNAc particles decreased the diastolic $[Ca^{2+}]_i$ in PAB myocytes, with a further significant decrease in the diastolic $[Ca^{2+}]_i$ in the S100A1-GlcNAc treated myocytes at 0.5 Hz compared with the empty-GlcNAc treated group.

GlcNAc nanoparticles modulate *O*-linked modification of cardiac proteins

To determine if GlcNAc nanoparticles could influence the post-translational state of cardiac proteins, we investigated glycosylation of SERCA2a, the RyR2 and PLB. Rat CMs were incubated with either vehicle (CTL), nondecorated particles (PK) or GlcNAc-decorated particles (PK-GlcNAc) for 2 h. SERCA2a, RyR2 and PLB proteins were immunoprecipitated from these cells with specific antibodies against these proteins and blotted with anti-*O*-GlcNAc to determine if treatment with GlcNAc-decorated particles could increase the amount of *O*-linked glcnacylation of these proteins *in vitro*. As shown in Figure 5, a basal level of *O*-GlcNAc is detected for SERCA2a (Figure 5A), RyR2 (Figure 5C) and PLB (Figure 5E) after vehicle treatment (CTL; upper panels). The level of *O*-GlcNAc modification of SERCA2a, the RyR2 or PLB was not significantly changed after treatment with nondecorated particles (PK; upper panels). However, after treatment with GlcNAc-decorated particles, an increase in the *O*-GlcNAc incorporated onto SERCA2a (Figure 5A) and the RyR2 (Figure 5C) is observed (PK-GlcNAc; upper panels). Conversely, no significant *O*-GlcNAc incorporation on PLB above basal levels was detected after treatment with PK-GlcNAc particles (Figure 5E). These results are quantified and summarized in Figure 5B, D & F. Our results indicate that direct GlcNAcylation of SERCA2a and not GlcNAcylation of PLB, which regulates SERCA2a function, may be the mechanism by which GlcNAc modulates SERCA2a in rat CMs. These data indicate that GlcNAc moieties decorating nanoparticles can be utilized intracellularly to modify key cardiac Ca^{2+} handling proteins and thus regulate their function.

Discussion

Delivery of small molecules to the heart is limited by the ability of CMs to internalize substances. We have previously described the development of a drug delivery system for enhanced CM uptake by decorating degradable, biocompatible, polyketal nanoparticles with GlcNAc and demonstrated their ability to be internalized by cardiac myocytes. In this study, we expand upon those observations by demonstrating not just internalization of nanoparticles in to failing CM, but also modulation of calcium handling due to the presence of GlcNAc in addition to the cargo protein S100A1. We show that GlcNAc moieties released from intracellular nanoparticle degradation can be used as a substrate for post-translational modification of calcium handling proteins in CMs, hence making it a 'bioactive' nanoparticle.

The cardiac Ca^{2+}-binding protein S100A1 has emerged as an attractive therapeutic target based on its interaction with key E-C coupling proteins [8–10], thus S100A1 has become the basis for ongoing preclinical trials for HF therapy [11,12]. One major limitation is that S100A1 is unable to cross the cell membrane and thus intracellular delivery remains a major hurdle. Current strategies employ viral-based cardiac gene therapy techniques for intracellular protein expression; however, the long-term biosafety of these therapies is an issue of concern. Furthermore, these approaches allow neither terminating nor adapting the level of the protein expression intracellularly. We have previously shown that utilization of GlcNAc nanoparticles represents a potential vehicle for small molecule delivery to CMs. Once internalized, these particles are degraded into the biocompatible

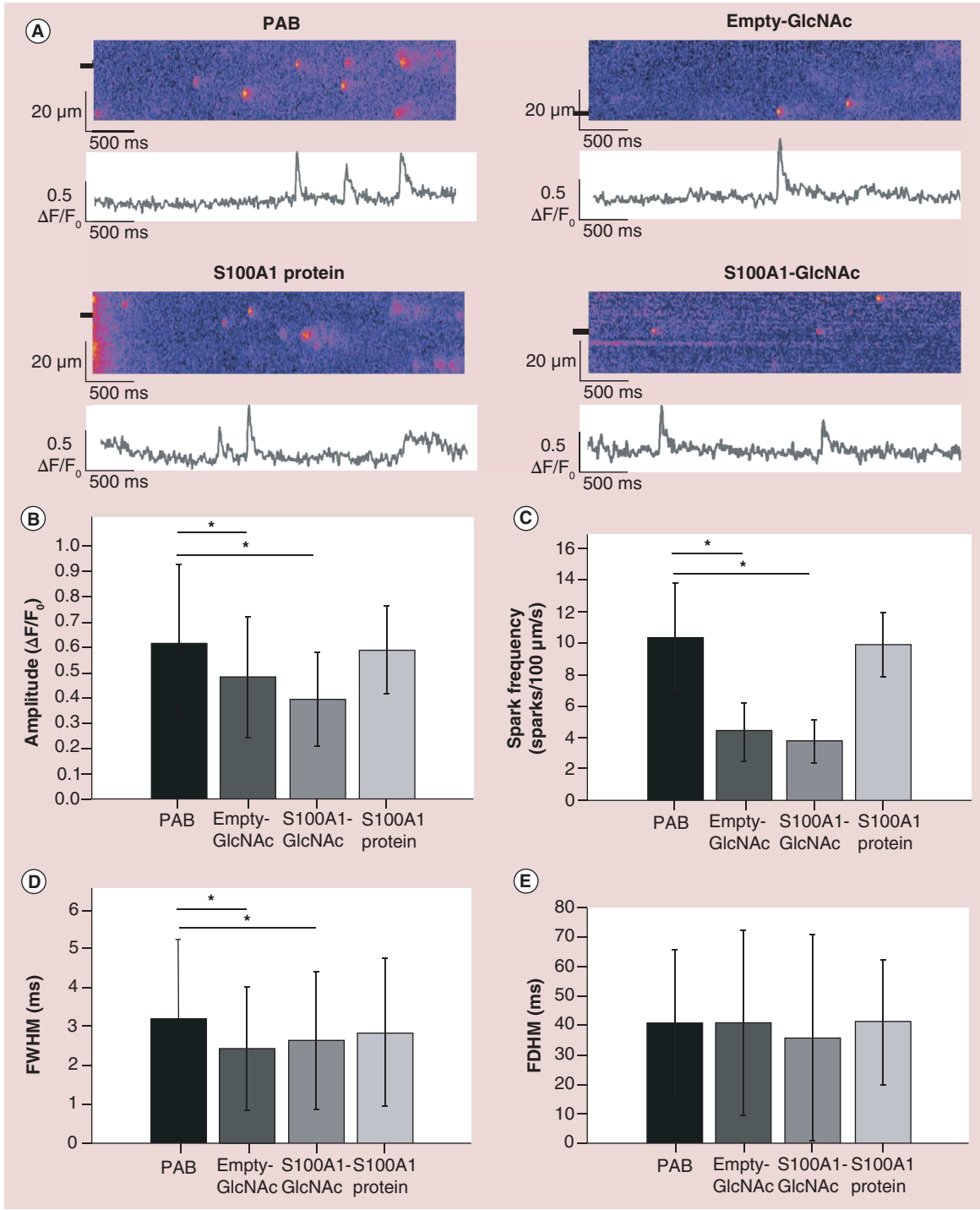

Figure 3. *N*-acetylglucosamine nanoparticle treatment alters the properties of Ca^{2+} sparks from intact right ventricular myocytes. **(A)** Representative line scans and the corresponding fluorescence profiles ($\Delta F/F_0$) of Ca^{2+} sparks from intact rat myocytes from PAB or PAB treated with empty GlcNAc nanoparticles (empty-GlcNAc), S100A1-loaded GlcNAc nanoparticles (S100A1-GlcNAc) or external S100A1 native protein. Fluorescent profiles were generated from the line scan regions marked by black boxes. **(B–D)** Summary data of the spark amplitude **(B)**, spark frequency **(C)**, FWHM; **(D)** and FDHM; **(E)** measured from the four groups. PAB: n = 176 sparks from n = 9 rats; Empty-GlcNAc: n = 119 sparks from n = 10 rats; S100A1-GlcNAc: n = 145 sparks from n = 11 rats; S100A1 protein: n = 39 sparks from n = 3 rats.
*$p < 0.05$.
FDHM: Full duration at half maximum; FWHM: Full width at half maximum; GlcNAc: *N*-acetylglucosamine; PAB: Pulmonary artery banded.

products, acetone and cyclohexanedimethanol, producing no acute toxicity to the cell [13]. Thus, our GlcNAc nanoparticles are a viable system for delivery of cargo proteins to CMs for therapeutic effects and also have the potential for dose-dependent delivery into the intact myocardium. Furthermore, the positive effects seen on

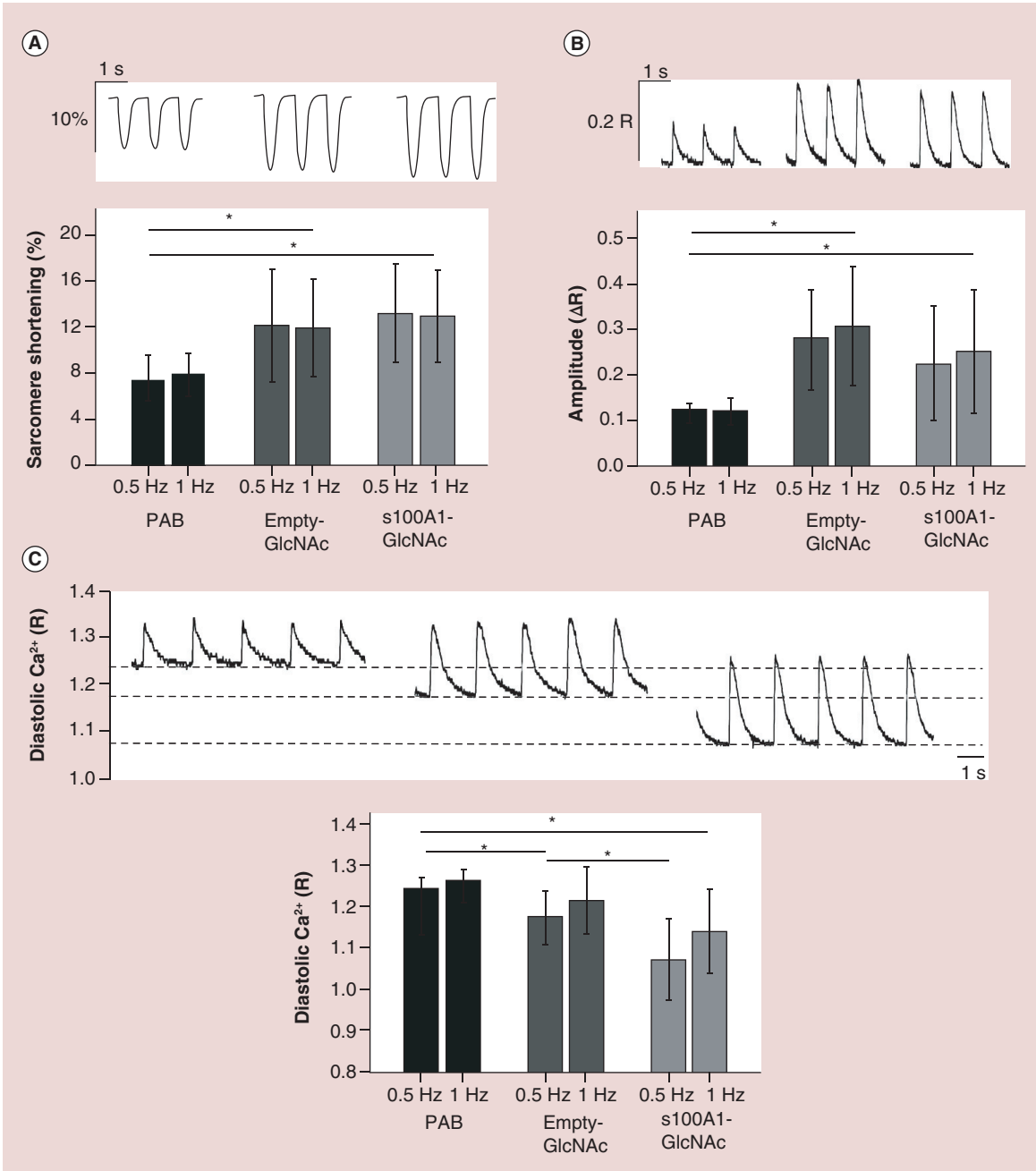

Figure 4. *N*-acetylglucosamine nanoparticle treatment restores sarcomere shortening, Ca^{2+} transient amplitude and decreases diastolic Ca^{2+} in pulmonary artery banded myocytes. (A) Representative sarcomere shortening, **(B)** Ca^{2+} transient amplitude and **(C)** diastolic Ca^{2+} traces from PAB, empty-GlcNAc treated and S100A1-GlcNAc treated myocytes during 0.5 and 1 Hz electrical stimulation. Summary bar graphs are shown for each parameter below the traces. Sarcomere shortening is shown as the percentage change in sarcomere length during contraction. Ca^{2+} transient amplitude (ΔR) and diastolic Ca^{2+} (R) measurements were made in cells loaded with 10 μM of the ratiometric Ca^{2+} indicator fura-2/AM. Representative traces are from cells during **(A & B)** 1.0 Hz or **(C)** 0.5 Hz stimulation. PAB: n = 8–13 cells from n = 6 rats; empty-GlcNAc: n = 9–13 cells from n = 6 rats; S100A1-GlcNAc: n = 8–12 cells from n = 6 rats.
*$p < 0.05$.
GlcNAc: *N*-acetylglucosamine; PAB: Pulmonary artery banded.

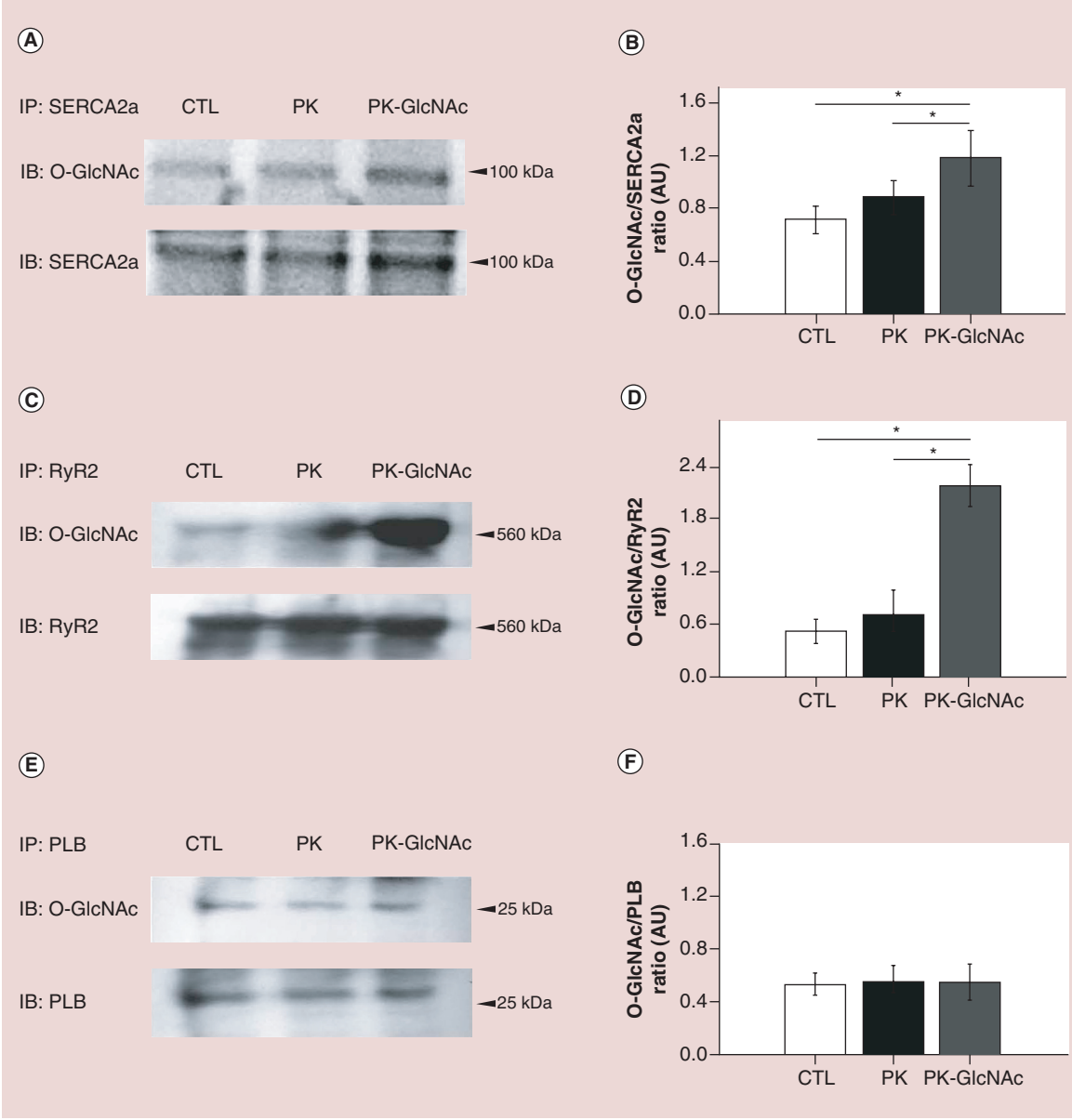

Figure 5. *N*-acetylglucosamine-decorated nanoparticles modulate *O*-linked GlcNAcylation of cardiac proteins.
Rat myocytes were incubated with vehicle, empty PK, or PK-GlcNAc for 2 h and proteins were harvested and lysates immunoprecipitated with anti-SERCA2a **(A)**, anti-RyR2 **(C)** or anti-PLB **(E)** antibodies and blotted for both *O*-GlcNAc (top panels) and immunoprecipitated target protein (bottom panels). Densitometry was used to quantify the western blot data and the results are shown in a summary bar graphs for n = 3 experiments for SERCA2a **(B)** the RyR2 **(D)**and PLB **(F)**.
*$p < 0.05$.
CTL: Control; GlcNAc: *N*-acetylglucosamine; PK: Particles.

other cells of the heart such as cardiac fibroblasts [21] and cardiac endothelial cells [22] with S100A1 therapy gives our GlcNAc delivery system the potential to be more comprehensive of a therapy that viral-based therapies that are engineered to specifically express in CMs.

In isolated CMs, GlcNAc nanoparticles reduced aberrant calcium release in failing CMs compared with undecorated particles. The decreased frequency of Ca^{2+} sparks in cells treated with S100A1-GlcNAc nanoparticles is consistent with reports of S100A1 binding to and stabilizing the RyR2 [23,24], thus less Ca^{2+} is released during spontaneous RyR2 openings and the openings become less frequent. This is illustrated by our observation of a decrease in the spark amplitude, the spark frequency and the spark FWHM. Furthermore, one mechanism for Ca^{2+} sparks in HF cells is instability in the channel structure induced by hyperphosphorylation of the RyR2 [25–28]. Thus, it is possible the decrease in

spark amplitude, frequency and FWHM seen in empty-GlcNAc treated cells compared with PAB is due to GlcNAcylation of the RyR2 competing with phosphorylation for modification of serine and threonine residues of the RyR2 and preventing the channel from becoming hyperphosphorylated and unstable. This is consistent with our data in Figure 5 showing that the RyR2 is *O*-GlcNAcylated following treatment with GlcNAc-decorated nanoparticles. Provided that Ca^{2+} sparks represent an arrhythmogenic substrate for the activation of Ca^{2+} waves [29], these results indicate an anti-arrhythmogenic effect of GlcNAc nanoparticles on HF myocytes. Additionally, interaction of S100A1 with mitochondria has been shown to regulate ATP production which may affect cellular energetics and also spark parameters in S100A1-GlcNAc treated CMs since ATP is a key modulator of both RyR2 and SERCA2a function. It is of note that treatment of CMs with native S100A1 protein had no significant effect on any of the parameters measured in the spark experiments, indicating that CMs do no efficiently uptake nonencapsulated S100A1 protein.

We also show that GlcNAc nanoparticles correct dysfunction in global Ca^{2+} handling and contractile function in PAB myocytes. Our data indicate that treatment of PAB myocytes with both empty-GlcNAc and S100A1-GlcNAc nanoparticles can improve the Ca^{2+} transient amplitude and contractility in electrically stimulated cells while also reducing the diastolic Ca^{2+} level. Additionally, we demonstrate a beneficial effect of S100A1-GlcNAc nanoparticles over empty particles in the reduction of diastolic Ca^{2+} levels in failing myocytes. The increased reduction in diastolic Ca^{2+} levels in failing myocytes seen with S100A1-GlcNAc treatment may provide additional protection from the incidence of arrhythmias due to Ca^{2+} overload in the intact heart [30]. The sarcomere shortening data support the hypothesis that S100A1 can interact with contractile proteins and alter their sensitivity to Ca^{2+} [12]. Furthermore, the increase in transient amplitude and the decrease in diastolic Ca^{2+} are consistent with previous reports of facilitating SR Ca^{2+} uptake by SERCA2a and decreased diastolic release events through the RyR2 [11,12,31–33].

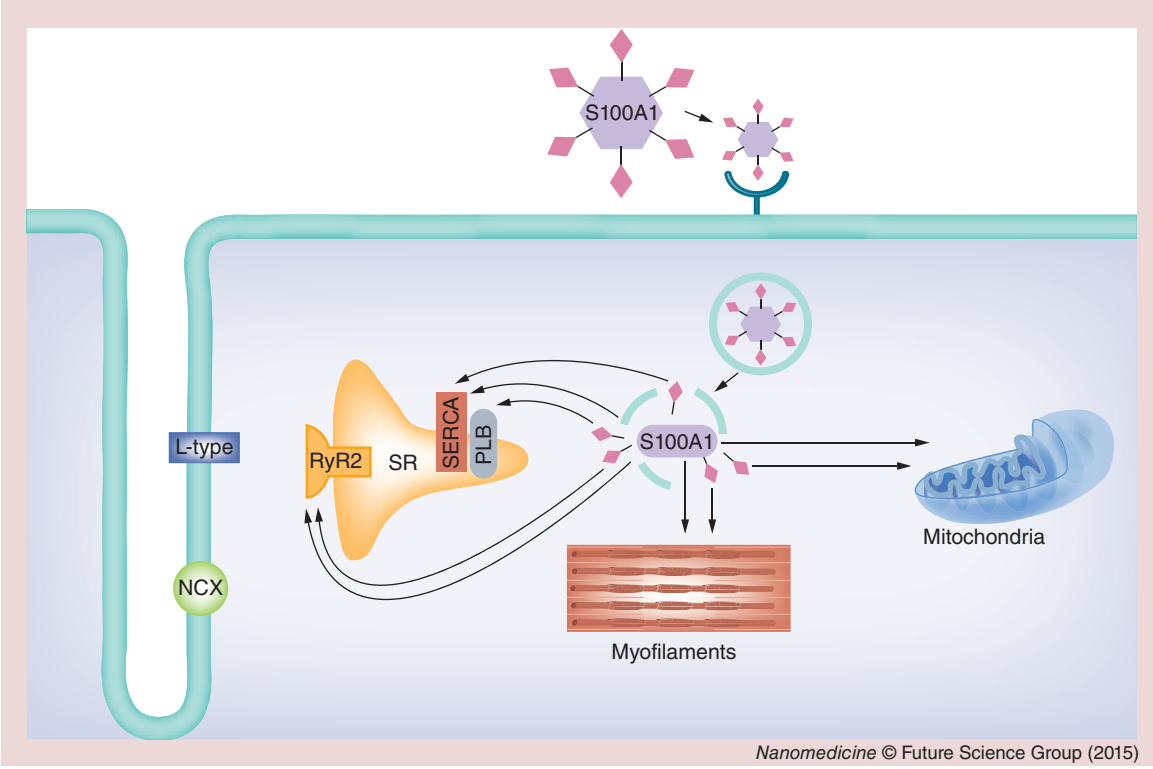

Figure 6. Illustration of the proposed mode of action of S100A1-*N*-acetylglucosamine nanoparticles in cardiac myocytes. Extracellularly applied *N*-acetylglucosamine (GlcNAc) nanoparticles bind to cell surface receptors such as lectins on cardiac myocytes via their GlcNAc moiety (pink diamonds) and then undergo receptor-mediated endocytosis for internalization into the cardiac myocytes. The nanoparticles are lysed in the acidic environment of the endosome, thus releasing the GlcNAc moieties and S100A1 cargo proteins. Degradation of the endosome releases GlcNAc and S100A1 protein into the cytosol where they are free to diffuse to their predicted target proteins (thin black arrows). Proposed target proteins of GlcNAc and S100A1 modulation include key Ca^{2+} handling proteins located on the SR, myofilaments and mitochondria.
L-type: L-type Ca^{2+} channel; NCX: Na^{+}/Ca^{2+} exchanger; PLB: Phospholamban; RyR2: Type 2 ryanodine receptor; SERCA: Sarcoplasmic/endoplasmic Ca^{2+}-ATPase.

Based on our experimental results, we propose a potential model shown in Figure 6 by which S100A1-GlcNAc nanoparticles modulate Ca^{2+} handling proteins in CMs. Based on previous studies, the GlcNAc moiety tethered to the surface of the nanoparticle is proposed to interact with lectins on the cell membrane of CMs [34–36]. We postulate that GlcNAc nanoparticles bind to cell surface receptors, specifically lectins, on CMs and undergo receptor-mediated endocytosis [37]. The nanoparticles are lysed in the acidic environment of the endosome, leaving behind the GlcNAc moiety and S100A1 cargo protein. The endosome degrades and releases GlcNAc and S100A1 protein into the cytosol where they are free to diffuse to their sites of action. The S100A1 protein can directly interact with and modulate its target proteins, while the GlcNAc is used as a substrate for *O*-linked glcnacylation of intracellular proteins. Post-translational modification of proteins by *O*-GlcNAc, much like protein phosphorylation, is an important regulatory mechanism in the modulation of signal cascades, metabolism and the stress response [38,39]. Modification of many cardiac proteins by *O*-GlcNAc has been shown [38], with effects on the interaction and function of these proteins [39]. The RyR2 has previously been shown to be modified by *O*-GlcNAC [40], while an increase in overall cardiac protein *O*-GlcNAc levels has been reported to be cardio-protective against ischemia-reperfusion injury in rat ventricular myocytes [41]. We hypothesize that the presence of GlcNAc on the empty nanoparticles elicits *O*-GlcNAcylation of intracellular proteins, thus resulting in the functional effects we observed with empty GlcNAc particles, however, the totality cardiac proteins that are modified by *O*-GlcNAc and the resulting effects on the function of these proteins is yet to be elucidated. Therefore, our proposed targets of GlcNAc and S100A1 modulation based on the results presented here and previously published reports include key Ca^{2+} handling proteins located on the SR membrane, mitochondria and myofilaments.

Conclusion

These data indicate that GlcNAc-decorated nanoparticles are a rapid and efficient delivery system for cardiac myocytes, and the GlcNAc nanoparticles themselves are biologically active and able to regulate the Ca^{2+} handling proteins in CMs. After treatment with either empty-GlcNAc or S100A1-GlcNAc nanoparticles, we observed a decrease in the amplitude and frequency of arrhythmogenic Ca^{2+} release in the form of Ca^{2+} sparks, an increase in electrically induced Ca^{2+} transient amplitude, an increase in cell shortening and a decrease in the diastolic Ca^{2+} in the cytosol. These data show that the nanoparticle is bioactive, however, there is also an additional effect of S100A1-GlcNAc nanoparticles on the diastolic Ca^{2+}. Thus, we report the development of a bioactive nanoparticle that provides a 'two-hit' treatment to CMs that can be utilized for further encapsulation of therapeutic molecules and proteins for delivery to failing myocytes while providing an additional beneficial effect by being utilized in post-translational modification of intracellular proteins.

Future perspective

We have shown in this report the therapeutic effects that empty-GlcNAc and S100A1-GlcNAc nanoparticles have on isolated primary CMs. Future studies will be aimed at determining the effect of S100A1-GlcNAc particles on heart function *in vivo*. Given that this study focused on the acute effects of empty-GlcNAc and S100A1-GlcNAc nanoparticles, it will be critical to determine the long-term effects of GlcNAc nanoparticles and also the time and dose dependence of S100A1 activity in the intact myocardium. This information will be critical in fine-tuning our nanoparticle delivery system to have the greatest therapeutic effect possible.

Acknowledgements

The authors would like to thank the Emory + Children's Pediatric Research Center Animal Physiology Core for surgical assistance and SK French for her contribution to the design of the model figure.

Financial & competing interests disclosure

This publication has been funded in whole or in part with the federal funds from the National Heart, Lung and Blood Institute, NIH, Department of Health and Human Services, under Contract No. HHSN268201000043C, as well as grant HL090601 to ME Davis and American Heart Association grant 11GRNT7490000 to MB Wagner. The authors also wish to acknowledge the support of the Children's Miracle Network gift to Children's Healthcare of Atlanta, funding from the Center for Pediatric Nanomedicine at Georgia Institute of Technology and Children's Healthcare of Atlanta. The authors have no other relevant affiliations or financial involvement with any organization or entity with a financial interest in or financial conflict with the subject matter or materials discussed in the manuscript apart from those disclosed.

No writing assistance was utilized in the production of this manuscript.

Ethical conduct of research

The authors state that they have obtained appropriate institutional review board approval or have followed the principles outlined in the Declaration of Helsinki for all human or animal experimental investigations. In addition, for investigations involving human subjects, informed consent has been obtained from the participants involved.

Executive summary

Background

- Delivery of small molecules to the heart is limited by the ability of cardiomyocytes (CMs) to internalize substances. Our laboratory has previously described the development of a small molecule delivery system for enhanced CM uptake by decorating degradable, biocompatible polymeric nanoparticles with *N*-acetylglucosamine (GlcNAc). Since GlcNAc can be used as a substrate to modify intracellular proteins, we hypothesize that GlcNAc nanoparticles will have a 'two-hit' effect on Ca^{2+} handling in CMs whereby the cargo and also the GlcNAc moiety itself modulates intracellular protein activity.

Aim

- To evaluate the ability of GlcNAc-decorated nanoparticles and their cargo to modulate calcium handling in failing CMs.

Approach

- We utilized CMs isolated from rats with right ventricular heart failure induced by pulmonary artery banding and assessed various physiological Ca^{2+} handling parameters.

Key findings

- GlcNAc decoration increases polymeric nanoparticle uptake in isolated failing cardiac myocytes.
- The small Ca^{2+} binding protein, S100A1, can be encapsulated into GlcNAc decorated nanoparticles and the protein retains its physiological function after nanoparticle degradation.
- After treatment with either empty-GlcNAc or S100A1-GlcNAc nanoparticles, we observed a decrease in the amplitude and frequency of arrhythmogenic Ca^{2+} release in the form of Ca^{2+} sparks.
- We recorded an increase in electrically induced Ca^{2+} transient amplitude, an increase in cell shortening and a decrease in the diastolic Ca^{2+} in the cytosol after treatment with either empty-GlcNAc or S100A1-GlcNAc nanoparticles.
- Treatment of CMs with GlcNAc nanoparticles can enhance *O*-linked GlcNAcylation of intracellular proteins.

Conclusion

- We report the development of a bioactive nanoparticle that provides a 'two-hit' treatment to CMs. Our nanoparticles can be utilized for further encapsulation of therapeutic molecules and proteins for delivery to CMs, while providing an additional beneficial effect by being utilized in post-translational modification of intracellular proteins.

References

Papers of special note have been highlighted as:
• of interest; •• of considerable interest

1 Lindner M, Erdmann E, Beuckelmann DJ. Calcium content of the sarcoplasmic reticulum in isolated ventricular myocytes from patients with terminal heart failure. *J. Mol. Cell. Cardiol.* 30(4), 743–749 (1998).

2 Pieske B, Maier LS, Bers DM, Hasenfuss G. Ca^{2+} handling and sarcoplasmic reticulum Ca^{2+} content in isolated failing and nonfailing human myocardium. *Circ. Res.* 85(1), 38–46 (1999).

3 Pogwizd SM, Schlotthauer K, Li L, Yuan W, Bers DM. Arrhythmogenesis and contractile dysfunction in heart failure: roles of sodium-calcium exchange, inward rectifier potassium current, and residual beta-adrenergic responsiveness. *Circ. Res.* 88(11), 1159–1167 (2001).

4 Shannon TR, Pogwizd SM, Bers DM. Elevated sarcoplasmic reticulum Ca^{2+} leak in intact ventricular myocytes from rabbits in heart failure. *Circ. Res.* 93(7), 592–594 (2003).

5 Guo T, Ai X, Shannon TR, Pogwizd SM, Bers DM. Intra-sarcoplasmic reticulum free [Ca^{2+}] and buffering in arrhythmogenic failing rabbit heart. *Circ. Res.* 101(8), 802–810 (2007).

6 Maxwell JT, Domeier TL, Blatter LA. Dantrolene prevents arrhythmogenic Ca^{2+} release in heart failure. *Am. J. Physiol. Heart Circ. Physiol.* 302(4), H953–H963 (2012).

7 George CH. Sarcoplasmic reticulum Ca^{2+} leak in heart failure: mere observation or functional relevance? *Cardiovasc. Res.* 77(2), 302–314 (2008).

8 Most P, Bernotat J, Ehlermann P *et al.* S100A1: a regulator of myocardial contractility. *Proc. Natl Acad. Sci. USA* 98(24), 13889–13894 (2001).

• **A key report establishing S100A1 as a critical regulator of myocardial contractility.**

9 Most P, Remppis A, Pleger ST *et al.* Transgenic overexpression of the Ca^{2+}-binding protein S100A1 in the heart leads to increased *in vivo* myocardial contractile performance. *J. Biol. Chem.* 278(36), 33809–33817 (2003).

10 Volkers M, Loughrey CM, Macquaide N *et al.* S100A1 decreases calcium spark frequency and alters their spatial characteristics in permeabilized adult ventricular cardiomyocytes. *Cell Calcium* 41(2), 135–143 (2007).

•• **Established S100A1 as a modulator of ryanodine receptor activity in the heart, specifically showing an effect on diastolic calcium release events such as calcium sparks.**

11 Pleger ST, Shan C, Ksienzyk J *et al.* Cardiac AAV9-S100A1 gene therapy rescues post-ischemic heart failure in a preclinical large animal model. *Sci. Transl. Med.* 3(92), 92ra64 (2011).

12 Brinks H, Rohde D, Voelkers M *et al.* S100A1 genetically targeted therapy reverses dysfunction of human failing cardiomyocytes. *J. Am. Coll. Cardiol.* 58(9), 966–973 (2011).

13 Gray WD, Che P, Brown M, Ning X, Murthy N, Davis ME. *N*-acetylglucosamine conjugated to nanoparticles enhances myocyte uptake and improves delivery of a small molecule p38 inhibitor for post-infarct healing. *J. Cardiovasc. Transl. Res.* 4(5), 631–643 (2011).

•• **Shows that *N*-acetylglucosamine decoration of nanoparticles enhances their uptake by cardiac myocytes.**

14 Marsh SA, Collins HE, Chatham JC. Protein *O*-GlcnAcylation and cardiovascular (patho)physiology. *J. Biol. Chem.* 289(50), 34449–34456 (2014).

15 Song X, Qian X, Shen M *et al.* Protein kinase C promotes cardiac fibrosis and heart failure by modulating galectin-3 expression. *Biochim. Biophys. Acta* 1853(2), 513–521 (2015).

16 Wang Y, Joyner RW, Wagner MB, Cheng J, Lai D, Crawford BH. Stretch-activated channel activation promotes early afterdepolarizations in rat ventricular myocytes under oxidative stress. *Am. J. Physiol. Heart Circ. Physiol.* 296(5), H1227–H1235 (2009).

17 Lee S, Yang SC, Heffernan MJ, Taylor WR, Murthy N. Polyketal microparticles: a new delivery vehicle for superoxide dismutase. *Bioconjug. Chem.* 18(1), 4–7 (2007).

•• **Shows the application of polyketal microparticles as a delivery vehicle for proteins and small molecules, paving the way for synthesis of polyketal nanoparticles for drug delivery.**

18 Sy JC, Seshadri G, Yang SC *et al.* Sustained release of a p38 inhibitor from non-inflammatory microspheres inhibits cardiac dysfunction. *Nat. Mater.* 7(11), 863–868 (2008).

19 Cheng H, Lederer WJ, Cannell MB. Calcium sparks: elementary events underlying excitation-contraction coupling in heart muscle. *Science* 262(5134), 740–744 (1993).

20 Volkers M, Loughrey CM, Macquaide N *et al.* S100a1 decreases calcium spark frequency and alters their spatial characteristics in permeabilized adult ventricular cardiomyocytes. *Cell Calcium* 41(2), 135–143 (2007).

21 Rohde D, Schon C, Boerries M *et al.* S100a1 is released from ischemic cardiomyocytes and signals myocardial damage via toll-like receptor 4. *EMBO Mol. Med.* 6(6), 778–794 (2014).

• **Presents the first evidence of the effect of S100A1 on other cardiac cells such as fibroblasts and endothelial cells when S100A1 is delivered to the intact myocardium.**

22 Most P, Lerchenmuller C, Rengo G *et al.* S100a1 deficiency impairs postischemic angiogenesis via compromised proangiogenic endothelial cell function and nitric oxide synthase regulation. *Circ. Res.* 112(1), 66–78 (2013).

23 Treves S, Scutari E, Robert M *et al.* Interaction of S100A1 with the Ca^{2+} release channel (ryanodine receptor) of skeletal muscle. *Biochemistry* 36(38), 11496–11503 (1997).

24 Wright NT, Prosser BL, Varney KM, Zimmer DB, Schneider MF, Weber DJ. S100A1 and calmodulin compete for the same binding site on ryanodine receptor. *J. Biol. Chem.* 283(39), 26676–26683 (2008).

25 Ai X, Curran JW, Shannon TR, Bers DM, Pogwizd SM. Ca^{2+}/calmodulin-dependent protein kinase modulates cardiac ryanodine receptor phosphorylation and sarcoplasmic reticulum Ca^{2+} leak in heart failure. *Circ. Res.* 97(12), 1314–1322 (2005).

26 Marx SO, Reiken S, Hisamatsu Y *et al.* PKA phosphorylation dissociates FKBP12.6 from the calcium release channel (ryanodine receptor): defective regulation in failing hearts. *Cell* 101(4), 365–376 (2000).

27 Reiken S, Gaburjakova M, Guatimosim S *et al.* Protein kinase a phosphorylation of the cardiac calcium release channel (ryanodine receptor) in normal and failing hearts. Role of phosphatases and response to isoproterenol. *J. Biol. Chem.* 278(1), 444–453 (2003).

28 Wehrens XH, Lehnart SE, Reiken SR, Marks AR. Ca^{2+}/calmodulin-dependent protein kinase II phosphorylation regulates the cardiac ryanodine receptor. *Circ. Res.* 94(6), e61–e70 (2004).

29 Bassani RA, Bers DM. Rate of diastolic Ca release from the sarcoplasmic reticulum of intact rabbit and rat ventricular myocytes. *Biophys. J.* 68(5), 2015–2022 (1995).

30 Thandroyen FT, Morris AC, Hagler HK *et al.* Intracellular calcium transients and arrhythmia in isolated heart cells. *Circ. Res.* 69(3), 810–819 (1991).

31 Most P, Boerries M, Eicher C *et al.* Distinct subcellular location of the Ca^{2+}-binding protein s100a1 differentially modulates Ca^{2+}-cycling in ventricular rat cardiomyocytes. *J. Cell Sci.* 118(Pt 2), 421–431 (2005).

32 Most P, Seifert H, Gao E *et al.* Cardiac S100A1 protein levels determine contractile performance and propensity toward heart failure after myocardial infarction. *Circulation* 114(12), 1258–1268 (2006).

33 Most P, Boerries M, Eicher C *et al.* Distinct subcellular location of the Ca^{2+}-binding protein S100A1 differentially modulates Ca^{2+}-cycling in ventricular rat cardiomyocytes. *J. Cell Sci.* 118(Pt 2), 421–431 (2005).

34 Aso S-I, Ise H, Takahashi M *et al.* Effective uptake of *N*-acetylglucosamine-conjugated liposomes by cardiomyocytes *in vitro*. *J. Control. Release* 122(2), 189–198 (2007).

35 Monsigny M, Roche A-C, Midoux P, Mayer R. Glycoconjugates as carriers for specific delivery of therapeutic drugs and genes. *Adv. Drug Deliv. Rev.* 14(1), 1–24 (1994).

36 Weis WI, Drickamer K. Structural basis of lectin-carbohydrate recognition. *Annu. Rev. Biochem.* 65(1), 441–473 (1996).

37 Ise H, Kobayashi S, Goto M *et al.* Vimentin and desmin possess GlcNAc-binding lectin-like properties on cell surfaces. *Glycobiology* 20(7), 843–864 (2010).

• **Established the basis for conjugation of *N*-acetylglucosamine to nanoparticles for binding, and endocytosis by cardiac myocytes expressing lectin on their cell surface.**

38 Marsh SA, Collins HE, Chatham JC. Protein *O*-GlcNAcylation and cardiovascular (patho)physiology. *J. Biol. Chem.* 289(50), 34449–34456 (2014).

39 Johnsen VL, Belke DD, Hughey CC *et al.* Enhanced cardiac protein glycosylation (*O*-GlcNAc) of selected mitochondrial proteins in rats artificially selected for low running capacity. *Physiol. Genomics* 45(1), 17–25 (2013).

40 Rengifo J, Gibson CJ, Winkler E, Collin T, Ehrlich BE. Regulation of the inositol 1, 4, 5-trisphosphate receptor type I by *O*-GlcNAc glycosylation. *J. Neurosci.* 27(50), 13813–13821 (2007).

41 Champattanachai V, Marchase RB, Chatham JC. Glucosamine protects neonatal cardiomyocytes from ischemia-reperfusion injury via increased protein *O*-GlcNAc and increased mitochondrial Bcl-2. *Am. J. Physiol. Cell Physiol.* 294(6), C1509–C1520 (2008).